Univerzitet u Beogradu
Publikacije Elektrotehničkog Fakulteta
Serija Tehnička fizika (1998), 33–46

WAVES IN RELATIVISTIC PLASMAS Part II: Wave propagation at an arbitrary angle with respect to the magnetic field

Lj. Nikolić and S. Pešić

"Vinča" Institute for Nuclear Sciences, Laboratory for Nuclear and Plasma Physics, P.O.B. 522, 11001 Belgrade, Yugoslavia

In the first part of the paper [3] and the present, second part, a fully relativistic description of waves propagating at an arbitrary angle to the steady magnetic field in thermal plasma is discussed. The numerical code that we have developed to solve the fully relativistic dispersion equation is used in a wide range of plasma parameters and wave propagation conditions. The results of this study confirm the previously reported ones obtained within the weakly relativistic approximation and complement them by new effects which are brought on by relativistic effects at high electron temperatures. Some of the observed wave propagation and absorption features may be attractive for future applications in devices with energetic electrons.

I Introduction

The physical understanding of the role of relativistic mass variation in the wave propagation in plasmas is quite satisfactory and the results obtained describe correctly the propagation characteristics and predict the scaling of the damping parameters. In general, the detailed description of the processes involved in relativistic plasmas requires a numerical approach. Given the complexity of the fully relativistic dielectric tensor, most of the previous quantitative evaluations of the wave propagation and absorption quantities have been done numerically within the weakly relativistic approximation. As known, the range of applicability of this approximation depends strongly on the electron temperature. The fully relativistic dispersion equation has been solved numerically only for perpendicular propagation of the extraordinary wave in relativistic thermal [1] and non-thermal plasmas [2] and recently, for both, the ordinary and extraordinary wave [3,4]. In order to verify the previously reported results on this problem and complement them in the fully relativistic temperature domain, we have solved numerically the fully relativistic dispersion equation in the frequency range covering the fundamental electron cyclotron (EC) frequency and its first few harmonics. The perpendicular component $N_\perp$ of the wave refractive index $\mathbf{N}$ is treated as a complex quantity which permits to obtain precise informations on the wave damping. In fact, the present paper completes our previous studies of perpendicular

wave propagation [3] by considering electromagnetic and quasi-electrostatic modes propagating at an arbitrary angle with respect to the steady magnetic field in relativistic thermal plasma.

The paper is organized as follows. In Section 2 we discuss the complete dispersion equation governing waves in homogeneous plasma confined by a steady magnetic field, and some special cases of wave propagation. In Section 3 we present solutions of the fully relativistic dispersion equation for various electron temperatures, plasma densities, magnetic fields and parallel wave refractive indexes $N_{||}$, indicating the propagation and absorption properties of obliquely propagating ordinary (O) modes. The analysis of the obtained results but this time for the extraordinary (X) and quasi-longitudinal (QL) modes, is presented in Section 4. The results are summarized and conclusions discussed in Section 5.

II Dispersion equation

The general form of the dispersion equation governing waves with circular frequency ω propagating in a homogeneous plasma, $\mathbf{N} = N_\perp \mathbf{e}_y + N_{||}\mathbf{e}_z$, confined by a steady magnetic field $\mathbf{B}_0 = B_0\mathbf{e}_z$ is given in the first part of the present paper [3]. Taking into account the symmetry relations $\epsilon_{xy} = -\epsilon_{yx}$, $\epsilon_{xz} = -\epsilon_{zx}$ and $\epsilon_{yz} = \epsilon_{zy}$ the dispersion equation (1) in [3] can be written as

$$\begin{aligned} & N_\perp^4\epsilon_{yy} + 2N_\perp^3 N_{||}\epsilon_{yz} + N_\perp^2(N_{||}^2(\epsilon_{yy}+\epsilon_{zz}) + \epsilon_{yz}^2 - \epsilon_{xy}^2 - \epsilon_{yy}(\epsilon_{xx}+\epsilon_{zz})) + \\ + \; & 2N_\perp N_{||}(N_{||}^2\epsilon_{yz} - \epsilon_{xx}\epsilon_{yz} - \epsilon_{xy}\epsilon_{xz}) + \epsilon_{yy}\epsilon_{xz}^2 - \epsilon_{xx}\epsilon_{yz}^2 + \epsilon_{zz}(\epsilon_{xy}^2 + \epsilon_{xx}\epsilon_{yy}) - \\ - \; & 2\epsilon_{xy}\epsilon_{xz}\epsilon_{yz} + N_{||}^2(\epsilon_{yz}^2 - \epsilon_{xz}^2) + N_{||}^2\epsilon_{zz}(N_{||}^2 - \epsilon_{xx} - \epsilon_{yy}) = 0 \; . \end{aligned} \tag{1}$$

The fact that dielectric tensor is non-Hermitian indicates that the dispersion equation (1) has to be considered as a complex equation. Since we are primarily interested in propagation and damping of waves (externally) launched at some (real) frequency ω, equation (1) here is treated as an expression for the functional dependence of the complex perpendicular component of the wave refractive index $N_\perp$ upon the dimensionless parameters $X = \omega_p^2/\omega^2$, $Y = \omega/\omega_c = \bar{\omega}^{-1}$, $\mu = mc^2/T$ and $N_{||}$ (ω_p and ω_c are the plasma and electron cyclotron frequency, respectively). We recall the convention used in the present paper of the index r denoting the real part of a complex quantity (e.g. $N_{\perp r} = \mathrm{Re}(N_\perp)$) and the index i denoting the imaginary part of a complex quantity (e.g. $N_{\perp i} = \mathrm{Im}(N_\perp)$).

Let us now briefly discuss some special cases of the dispersion equation (1).

- Case $N_\perp = 0$. Using the formula [5]

$$J_\mu(z)J_\nu(z) = \frac{2}{\pi}\int_0^{\pi/2} J_{\mu+\nu}(2z\cos\theta)\cos\left[(\mu-\nu)\,\theta\right]d\theta \; , \quad \mathrm{Re}(\mu+\nu) > -1$$

for parallel propagation with respect to the magnetic field $\mathbf{B}_0$, we obtain $\epsilon_{xz} = \epsilon_{yz} = 0$ and the dispersion equation simplifies. Generally, two fundamental modes exist: the "right-handed" and "left-handed" wave. Since the O wave goes over into the "left-handed" wave, the dispersion equation of interest is

$$\epsilon_{zz}\,|_{N_\perp=0} = 1 - \frac{\mu^2 X}{2K_2(\mu)}\int_{-1}^{1}\frac{\tilde{u}^2 d\tilde{u}}{(1-N_{||}\tilde{u})^4}\int_{\bar{\omega}^*_{\min}}^{\infty} e^{-\mu\frac{\bar{\omega}^*}{(1-N_{||}\tilde{u})}}\bar{\omega}^{*2}d\bar{\omega}^* = 0 \; , \tag{2}$$

where $\bar{\omega}^* = \omega^*/\bar{\omega}$ and $\omega^*_{\min} = \bar{\omega}(1-N_{||}\tilde{u})/(1-\tilde{u}^2)^{1/2}$. From equation (2) we conclude that for parallel propagation $N_{||} \neq 0$ and $N_\perp = 0$ the "left-handed" wave does not interact with electrons. For the extraordinary wave and $N_\perp = 0$ the dispersion equation is just

$$\left(\epsilon_{xx}\,|_{N_\perp=0} - N_{||}^2\right)^2 + \epsilon_{xy}^2\,|_{N_\perp=0} = 0, \tag{3}$$

where

$$\epsilon_{xx}\mid_{N_\perp=0} = 1-\frac{\mu^2XY}{4K_2(\mu)}\int_{-1}^{1}\frac{d\tilde{u}}{(1-N_{||}\tilde{u})^2}\int_{\omega^*_{\min}}^{\infty}\left(\frac{\omega^{*2}}{\omega^{*2}_{\min}}-1\right)\frac{\omega^{*2}e^{-\mu Y\frac{\omega^*}{(1-N_{||}\tilde{u})}}}{\omega^{*2}-1}d\omega^* \qquad (4)$$
$$+ \; i\frac{\pi\mu^2XY}{8K_2(\mu)}\int_{-1}^{1}\frac{d\tilde{u}}{(1-N_{||}\tilde{u})^2}\int_{\omega^*_{\min}}^{\infty}\left(\frac{\omega^{*2}}{\omega^{*2}_{\min}}-1\right)\delta(\omega^*-1)e^{-\mu Y\frac{1}{(1-N_{||}\tilde{u})}}d\omega^*,$$

$$\epsilon_{xy}\mid_{N_\perp=0} = i\frac{\mu^2XY}{4K_2(\mu)}\int_{-1}^{1}\frac{d\tilde{u}}{(1-N_{||}\tilde{u})^2}\int_{\omega^*_{\min}}^{\infty}\left(\frac{\omega^{*2}}{\omega^{*2}_{\min}}-1\right)\frac{\omega^{*}e^{-\mu Y\frac{\omega^*}{(1-N_{||}\tilde{u})}}}{\omega^{*2}-1}d\omega^* \qquad (5)$$
$$+ \; \frac{\pi\mu^2XY}{8K_2(\mu)}\int_{-1}^{1}\frac{d\tilde{u}}{(1-N_{||}\tilde{u})^2}\int_{\omega^*_{\min}}^{\infty}\left(\frac{1}{\omega^{*2}_{\min}}-1\right)\delta(\omega^*-1)e^{-\mu Y\frac{1}{(1-N_{||}\tilde{u})}}d\omega^*.$$

- Case $N_\perp = N_{||} = 0$ (no wave propagation; see also, [1] and [6]). Putting in equations (2)-(5) $N_{||} = 0$ we can obtain the relativistic expressions for the true ordinary,

$$\epsilon_{zz}\mid_{N_\perp=N_{||}=0} = 1-\frac{\mu^2X}{3K_2(\mu)}\int_0^\infty\frac{\bar{p}^4}{\gamma^2}e^{-\mu\gamma}d\bar{p}=0, \qquad (6)$$

$\left(\bar{p}=p/mc, \gamma=(1-v^2/c^2)^{-1/2}\right)$ and extraordinary ($Y<1$) wave cutoff,

$$\left(\epsilon_{xx}^2+\epsilon_{xy}^2\right)_{N_{||}=N_\perp=0}=0, \qquad (7)$$

$$\epsilon_{xx}\mid_{N_\perp=N_{||}=0} = 1-\frac{\mu^2X}{3K_2(\mu)}\int_0^\infty\frac{\bar{p}^4}{\bar{p}^2+1-Y^2}e^{-\mu\gamma}d\bar{p}, \qquad (8)$$

$$\epsilon_{xy}\mid_{N_\perp=N_{||}=0} = i\frac{\mu^2XY}{3K_2(\mu)}\int_0^\infty\frac{\bar{p}^4}{\gamma(\bar{p}^2+1-Y^2)}e^{-\mu\gamma}d\bar{p}. \qquad (9)$$

Note that equations (2)-(9) may be used to determine the densities X_c at which there is no perpendicular wave propagation (for $N_{||}\neq 0$, equations (2)-(5)) and at which the wave does not propagate at all (equations (6)-(9)). The attention of this paper is focused to the case of oblique wave propagation $N_{||}\neq 0$ (including the special case $N_{||}\neq 0$, $N_\perp = 0$), when the complete dispersion equation (1) must be solved. The perpendicular wave propagation $N_{||}=0$ (including the special case $N_{||}=0$, $N_\perp=0$) is treated in the first part of the present paper [3]. For reasons of comparison some of these results will be also displayed here.

The dispersion equation (1) of waves propagating obliquely to the magnetic field with the dielectric tensor element $\epsilon_{ij}\equiv\epsilon_{ij}(X,Y,\mu,N_{||},N_\perp)$ is solved numerically by standard root-finding techniques in a wide range of plasma parameters. The numerical code is checked in the low, weakly relativistic and fully relativistic electron temperature ranges. At low temperatures ($T\leq 10$ eV) the obtained results coincide with the results of the cold plasma theory. In order to compare the present results with those obtained within the weakly relativistic approximation, we have developed a code in which the dielectric tensor is expressed through the weakly relativistic dispersion function. It should be noted that in this code, finite Larmor radius terms are retained up to third order. In the weakly relativistic range of temperatures ($T\leq 20$ keV) an excellent agreement between the results obtained by the fully and weakly relativistic codes, is found. Finally, the results obtained in the fully relativistic range ($T\geq 300$ keV) show features which are physically justifiable.

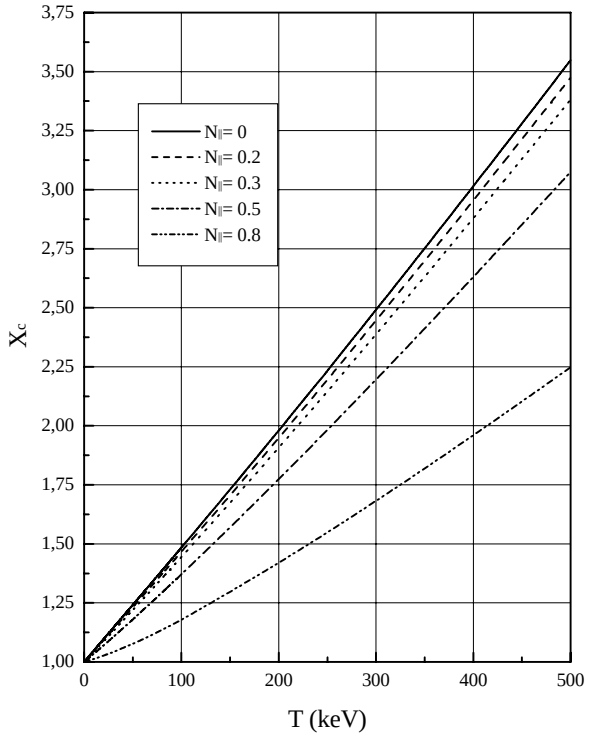

FIG. 1. Cutoff density X_c of the ordinary mode versus the electron temperature T for $N_{||} = 0$, $N_{||} = 0.2$, $N_{||} = 0.3$, $N_{||} = 0.5$ and $N_{||} = 0.8$.

III Ordinary mode

As is well known, in the cold plasma limit there are two cutoff densities for the O mode propagation: $X_c = 1$ for $N_{||}^2 \leq Y(1+Y)$ and the left-hand, high-density cutoff for $Y(1+Y) < N_{||}^2 < 1$. In what follows we shall be interested only in the plasma cutoff, $X_c = 1$. So, in cold plasma for $N_{||}^2 \leq Y(1+Y)$ there is no propagation of the O mode for frequencies below ω_p. At oblique wave propagation in thermal relativistic plasma the cutoff density depends on the electron temperature and parallel component of the wave refractive index $N_{||}$. For increasing the electron temperature it increases significantly. As in the case of perpendicular propagation [3] the cutoff density of the O mode may reach very high values. This is illustrated in Fig. 1 where we present the variation of the cutoff density X_c with the electron temperature for various values of $N_{||}$. This important increase of the cutoff density indicates that relativistic effects have to be taken into account when analyzing the results of microwave reflectometry in high-temperature plasmas. As one can see, for increasing $N_{||}$ the cutoff density decreases. The variation of X_c with $N_{||}$ is less pronounced in the range of large $N_{||}$ - values ($N_{||} \geq 0.5$).

The propagation and absorption properties of the O mode are depicted on Figs. 2-4 on which we show the variations of the real $N_{\perp r}$ and imaginary $N_{\perp i}$ part of the wave refractive index with Y around the fundamental EC frequency and its first few harmonics for $X = 0.3$, $T = 20$ keV (Fig. 2), $T = 100$ keV (Fig. 3) and $T = 300$ keV (Fig. 4), and several $N_{||}$ - values. The curves represented on Figs. 2-4 reveals that the so-called relativistic and Doppler regimes of EC wave propagation can not be separated clearly by some distinguishing features. Namely, in evaluating the propagation and absorption properties two regimes are usually distinguished: the Doppler (nonrelativistic regime), relevant to oblique propagation at sufficiently large angles with respect to the magnetic field $N_{||}^2 \gg \max\left(\left|\frac{n\omega_c}{\omega} - 1\right|, \frac{T}{mc^2}\right)$, and quasi-perpendicular (relativistic regime) $N_{||}^2 \ll \min\left(\left|\frac{n\omega_c}{\omega} - 1\right|, \frac{T}{mc^2}\right)$. The represented curves demonstrate that the wave propagation properties are similar in both regimes. A clear difference between these regimes can be observed only in the wave absorption properties, or

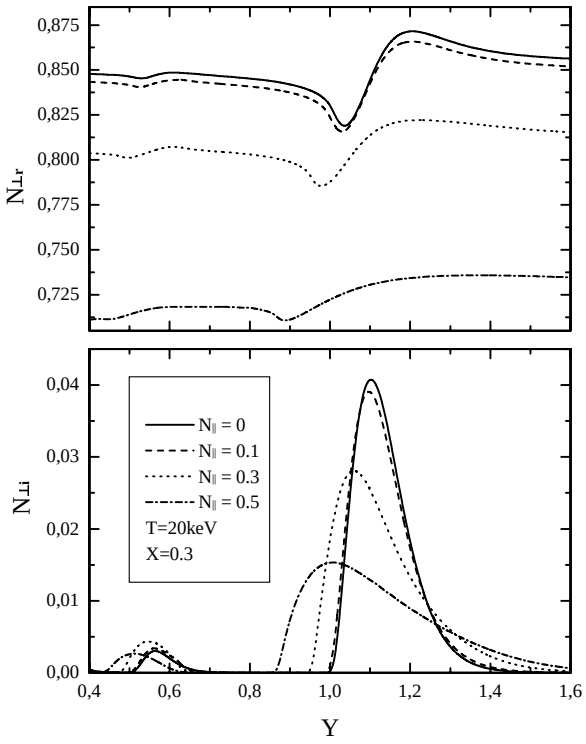

FIG. 2. The real ($N_{\perp r}$) and imaginary ($N_{\perp i}$) part of the ordinary wave refractive index versus Y for $T = 20$ keV, $X = 0.3$ and $N_{||} = 0$, $N_{||} = 0.1$, $N_{||} = 0.3$ and $N_{||} = 0.5$.

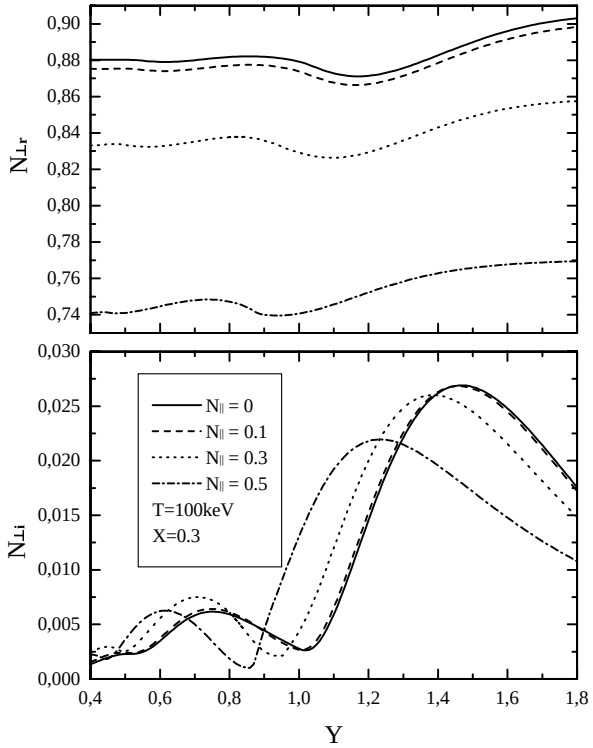

FIG. 3. As in Fig. 2 for $T = 100$ keV.

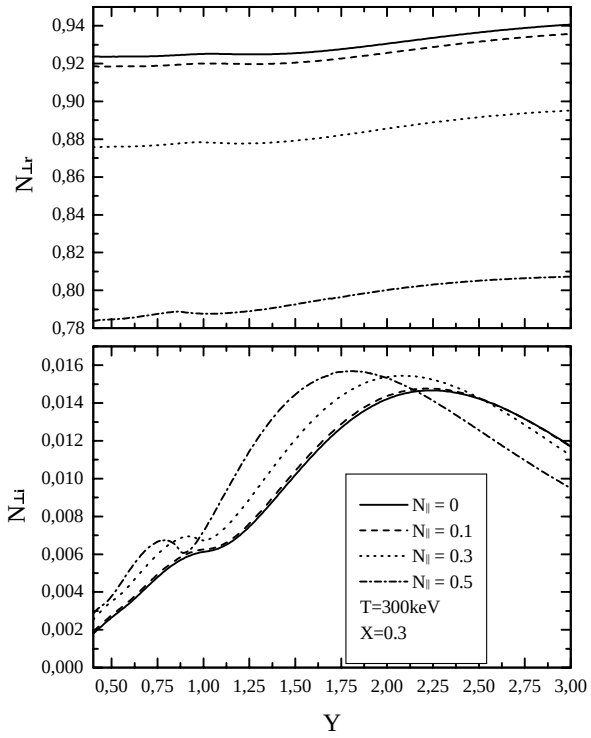

FIG. 4. As in Fig. 2 for $T = 300$ keV.

more precisely, in the wave absorption profiles. Furthermore as in the case of perpendicular wave propagation, near the ECR the real part of the wave refractive index varies strongly. Namely, near the resonance two marked extrema appear. In fact these two points represent branch points in the O wave propagation. At relatively low electron temperatures this anomalous wave behaviour is very pronounced. For increasing the electron temperature the frequency range in which the "wiggle" occurs, gradually enlarges. Finally, in the high-temperature, fully relativistic domain, the anomalous wave dispersion disappears (see for instance, Fig. 4). As $N_{||}$ is increased the effect of anomalous wave dispersion becomes less pronounced. The effect of anomalous wave dispersion occurs also at the second EC harmonic. However, there it is less pronounced.

The damping of O waves propagating obliquely in thermal relativistic plasma is efficient. The maximum value of the imaginary part of the wave refractive index $N_{\perp i}$ attains relatively high values ($N_{\perp i} \leq N_{\perp r}/10$). As expected, at low electron temperatures the absorption profiles show a harmonic structure which as the electron temperature increases, gradually transforms into a quasi-continuous spectrum. For increasing the electron temperature, the maxima of the imaginary part of the wave refractive index $N_{\perp i}$ broaden and displace towards higher Y -values. On the contrary the increase of $N_{||}$ shifts the maximum of $N_{\perp i}$ towards the ECR, $Y = 1$. It is interesting to note that at lower electron temperatures the increase of $N_{||}$ increases the maximum value of $N_{\perp i}$ while in the fully relativistic temperature domain ($T \geq 300$ keV) the variation of $N_{\perp i}$ with $N_{||}$ is less pronounced. The absorption properties of the O mode at the second EC harmonic differ from those discussed above. As $N_{||}$ is increased, the maximum value of $N_{\perp i}$ at first enlarges and after that it decreases. Here also, the absorption peak is located far from the exact resonance. Only at relatively low electron temperatures ($T \leq$ 20 keV), the maximum value of $N_{\perp i}$ is placed close to the second EC harmonic.

Let us now examine how the previously discussed propagation and absorption properties depend on the electron density X. In general, the real part of the wave refractive index $N_{\perp r}$ monotonously decreases with increasing the electron density. On the other hand, with increasing X the imaginary part of the wave refractive index $N_{\perp i}$ starts to increase up to a broad maximum occurring at large X-values ($X \geq$ 0.5). This behaviour is illustrated by Figs. 5-6 on which we show the variation of

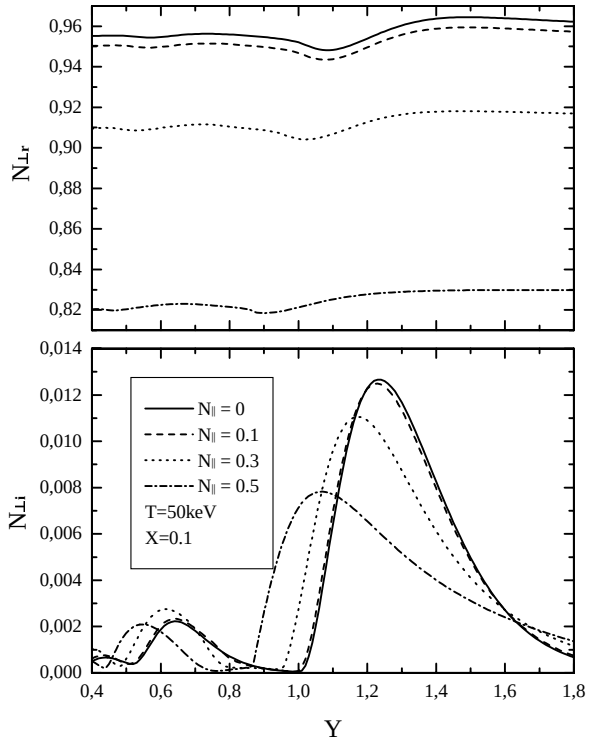

FIG. 5. The real ($N_{\perp r}$) and imaginary ($N_{\perp i}$) part of the ordinary wave refractive index versus Y for $T = 50\ keV$, $X = 0.1$ and $N_{||} = 0$, $N_{||} = 0.1$, $N_{||} = 0.3$ and $N_{||} = 0.5$.

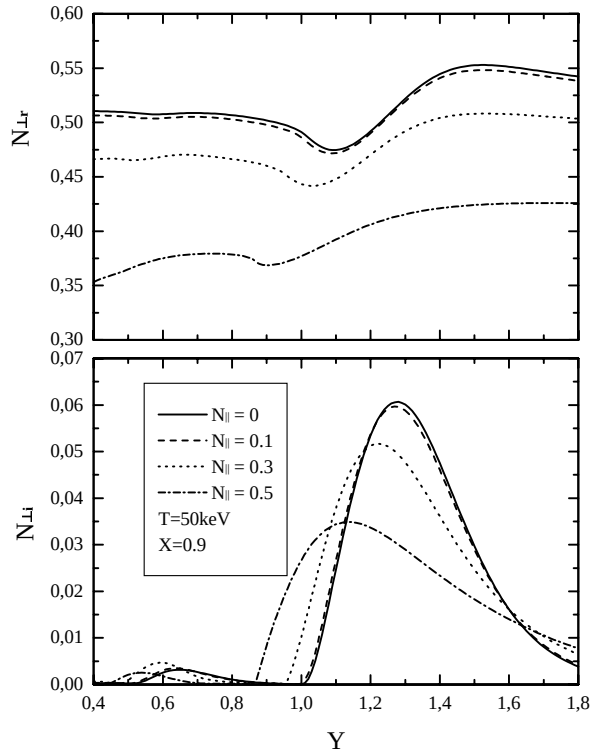

FIG. 6. As in Fig. 5 for $X = 0.9$.

$N_{\perp r}$ and $N_{\perp i}$ with Y for $T = 50$ keV, several values of $N_{||}$, and $X = 0.1$ (Fig. 5) and $X = 0.9$ (Fig. 6). As one can see, at $X = 0.1$ the effect of anomalous wave dispersion at the fundamental and second harmonic of the EC frequency is not pronounced. Namely, for $X = 0.1$ and $T = 50$ keV the plasma contribution to the dielectric tensor reduces and (depending on the value of $N_{||}$) the plasma refractive properties become relatively weak. The absorption profiles of the O mode at $X = 0.1$ and $X = 0.9$ have a similar structure but the damping is much weaker at low density.

IV Extraordinary and quasilongitudinal modes

As already noted, the dispersion relation (1) is treated as an equation for the functional dependence of the perpendicular component of the wave refractive index $N_\perp$ upon the parameters X, Y, μ and $N_{||}$. The parallel component of the wave refractive index $N_{||}$ which is usually fixed by boundary conditions, is considered as real quantity. Since we are studying waves propagating in plasma whose equilibrium particle-distribution function is stable, the obtained solutions have always a positive sign of $N_{\perp i} \geq 0$. In general, the considered waves are nonhomogeneous plane waves, $\exp i(\mathbf{Nr} - ct)\omega/c)$. The sign of the real part of the perpendicular wave refractive index $N_{\perp r}$ may be positive or negative describing forward or backward waves, respectively. Furthermore, at the low field side of the ECR there is a parameter range in which complex conjugate solutions of the dispersion relation are obtained.

As known, in magnetized thermal plasma two long-wavelength modes and a large number of short-wavelength modes can propagate. In this part of the paper we shall present the results concerning the propagation and absorption properties of the long wavelength mode which goes continuously into the fundamental electromagnetic X mode at low temperature. When $N_{||} = 0$ the wave electric field of this mode is perpendicular to the equilibrium magnetic field. Varying the parallel wave refractive index continuously from 0 to 1, the X mode goes over into the so-called right-handed mode. The X mode is more strongly coupled to the plasma than the previously considered O mode. On the other side, most of the short wavelength modes are heavily damped and consequently, of little practical interest. Here, we shall be interested only in the least damped short wavelength mode. Because of its nature this mode will be referred to as quasi-longitudinal (QL) mode. As we shall see later, these two modes can interchange. For this reason, in all figures that illustrate our discussion, the solutions are labelled by N_1 and N_2. Namely, the solution trajectory which at the low field side of the second harmonic of the EC frequency ($Y < 0.5$) starts as an X mode is displayed by full line and labelled by N_1, while the solution that starts as a highly damped QL mode is displayed by dashed line and labelled by N_2.

Two cutoff frequencies and two resonance frequencies characterize the range of the X mode propagation in cold plasma: the low- and high-density cutoff frequencies and the upper and lower hybrid frequencies. Since we are interested in the X mode propagation and absorption features around the EC frequency and its harmonics, we shall be mainly concerned with the low-density cutoff $X_c = (1 - N_{||}^2)(1 - Y)$ and the upper hybrid resonance $X_r + Y^2 = 1$. As known, the low-density cutoff is also referred to as right-hand cutoff as the wave polarization here is right-handed circular, that is the gyration of the wave field vector is in direction of the electron motion. The high-density cutoff takes place for $N_{||}^2 < Y/(1+Y) < 1$ at $X_c = (1-N_{||}^2)(1+Y)$ or for $Y > 1$ and $Y/(1+Y) \leq N_{||}^2 < 1$ at $X_c = 1$ while the lower hybrid resonance takes place out of the frequency range of interest.

In thermal plasma the location of the low-density cutoff depends also on the electron temperature. The temperature dependence of the low-density cutoff is shown on Fig. 7 on which we represent the variation of X_c with the electron temperature T for (a) $N_{||} = 0$, (b) $N_{||} = 0.2$ and (c) $N_{||} = 0.4$ and $Y = 0.7, Y = 0.8$ and $Y = 0.9$. Starting from its cold-plasma value the cutoff density increases almost linearly with the electron temperature. The cutoff density attains very high values: at $T = 140$ keV for example, X_c may reach six times its cold-plasma value. The largest increase of X_c takes place near the ECR and/or for perpendicular wave propagation. With increasing $N_{||}$, the temperature variation of the cutoff density reduces.

In the first part of the present paper [3] we have seen that at perpendicular wave propagation [7,8] near the fundamental and second harmonic of the EC frequency, the X and QL modes can interact. In

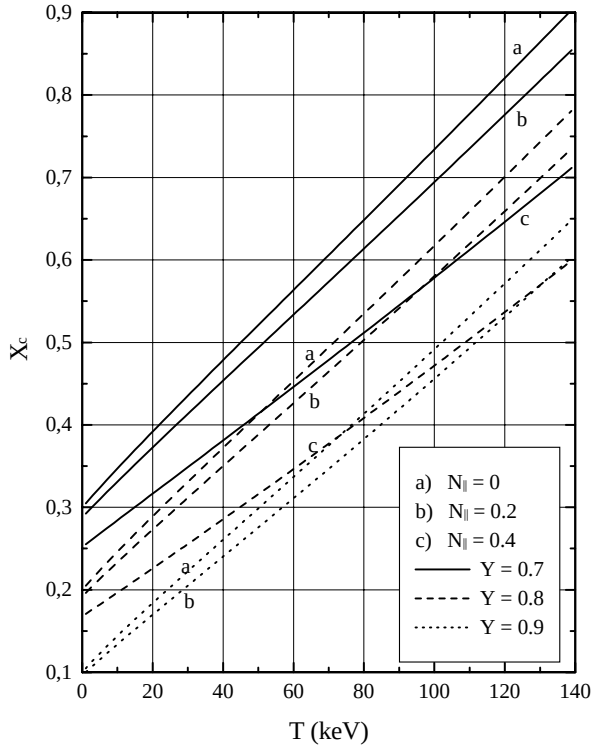

FIG. 7. Low-density cutoff of the extraordinary mode versus the electron temperature T for (a) $N_{||} = 0$, (b) $N_{||} = 0.2$ and (c) $N_{||} = 0.4$ and $Y = 0.7, Y = 0.8$ and $Y = 0.9$.

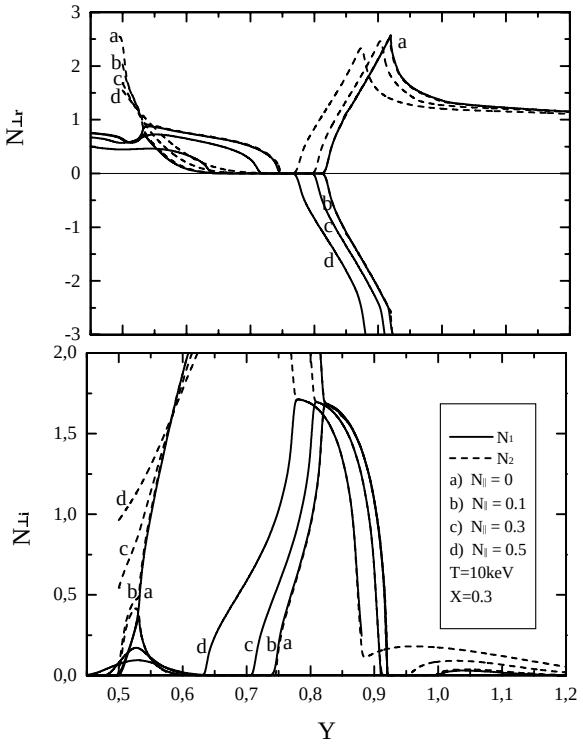

FIG. 8. The real ($N_{\perp r}$) and imaginary ($N_{\perp i}$) part of the X and QL modes versus Y for $X = 0.3$, several values of $N_{||}$, and $T = 10$ keV.

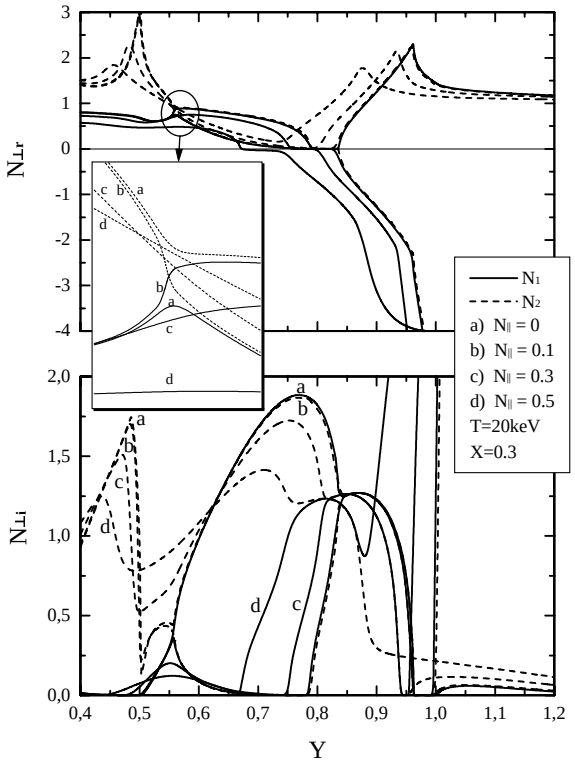

FIG. 9. As in Fig. 8 for $T = 20$ keV.

previous theoretical studies (see for instance [9]) it has been shown that mode interaction can occur also at oblique wave propagation. It should be noted that these studies were performed within the weakly relativistic dispersion approximation. The parameter which weighs the influence of mode interaction is $\gamma = X/\mu^{1/2} N_{||} Y^2$ [9]. At $\gamma = \gamma_c \simeq \mathcal{O}(1)$ the X and QL mode coalesce. For $\gamma < \gamma_c$ the aforementioned two modes propagate independently while for $\gamma > \gamma_c$ the low- and high-frequency branches of these modes interchange and mode coupling occurs: the high frequency QL mode matches smoothly with low-frequency X mode while the high-frequency X mode links with the solution trajectory of the highly damped QL mode. This physical picture is confirmed in the present study only in a limited temperature range. In Figs. 8-9 we show the real and imaginary parts of the X mode and the least damped QL mode which represent the solutions of the fully relativistic dispersion equation (1). In fact, the variations of $N_{\perp r}$ and $N_{\perp i}$ with Y for $X = 0.3$, several values of $N_{||}$, $T = 10$ keV and $T = 20$ keV, respectively, are shown in these figures. We see that an efficient damping of the nonconverted X modes occurs near the second EC harmonic and that the absorption profiles have a resonant structure. In agreement with the results obtained within the weakly relativistic approximation in both cases mode coupling occurs for $N_{||} = 0$. Mode coupling occurs also for $X = 0.3$ in the range $N_{||} \leq 0.07$ at $T = 20$ keV, and $N_{||} \leq 0.05$ at $T = 25$ keV (these cases are not represented). However at higher electron temperatures this phenomenon disappears (for instance, for $X = 0.3$ there is no mode coupling at $T = 30$keV). So, although the mode interaction is induced by relativistic effects, and consequently by finite-temperature effects, it takes place only in a limited range of relatively low temperatures (for $X = 0.3$ at $T < 30$ keV). Going back to the solutions represented in Figs. 8-9, we note that the converted X modes are highly damped. With increasing Y, the nonconverted X modes encounter the right-hand cutoff. After the location of the right-hand cutoff region in which these modes are evanescent ($N_{\perp r} = 0, N_{\perp i} \neq 0$) establishes. On the other side, the QL modes as well as the converted X modes are heavily damped in this parameter range.

Going further in the direction of increasing Y, one encounters a region in which complex conjugate solutions of the dispersion relation are obtained. The boundaries of this region are marked by Y_a and

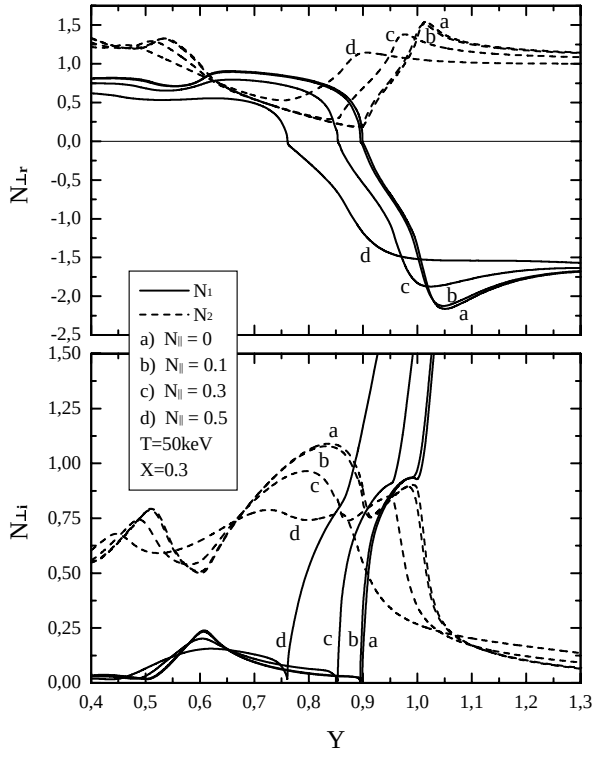

FIG. 10. As in Fig. 8 for $T = 50$ keV.

Y_b. Note that for $Y \geq Y_a$ the converted X mode behaves as an ordinary QL mode and vice versa, the QL mode behaves as an X mode. As $N_{||} \to 0$ the lower boundary of this region Y_a tends to the location of the upper hybrid resonance $Y_r = (1 - X)^{1/2}$. As $Y \to Y_b$, the imaginary part of the perpendicular component of the wave refractive index $N_{\perp i}$ (which is large at $Y = Y_a$), abruptly decreases so that at $Y = Y_b$, it becomes small. At $Y = Y_b$ sharp peaks of $N_{\perp r}$ of both, the QL modes and the converted X mode are formed. After the peak, the solution trajectory of these modes joins smoothly the classical solution. Simultaneously, a broad absorption profile near the ECR appear. The maximum value of $N_{\perp i}$ increases with increasing $N_{||}$, but in general, it is relatively low. The described features reveals that relativistic effects change significantly the classical physical picture of X mode propagation and absorption near the fundamental and second harmonic of the EC frequency.

In the intermediate temperature range 50 keV $\leq T \leq$ 100 keV the previously presented physical picture changes. The mode coupling near the second EC harmonic, the right-hand cutoff and the associated evanescent region of the (nonconverted) X modes disappear. To illustrate the wave propagation and absorption in this temperature range we have shown in Figs. 10-11 the variation of $N_{\perp r}$ and $N_{\perp i}$ with Y for $T = 50$ keV, several values of $N_{||}$ and $X = 0.3$ (Fig. 10) and $X = 0.1$ (Fig. 11). We see that both solutions are efficiently damped near the second EC harmonic. In the frequency range between the second and fundamental harmonic, the solution labelled N_1 changes sign. Note that the location at which N_1 changes sign is not a true cutoff ($N_{\perp r} = 0, N_{\perp i} = 0$). The solution labelled N_1 becomes a highly damped backward wave. The region of complex conjugate solutions of the dispersion relation still exists but now its lower boundary Y_a is located at $N_{\perp r} \neq 0$. At $Y = Y_a$ the imaginary part of the perpendicular component of the wave refractive index $N_{\perp i}$ of the N_1 mode starts to increase abruptly while the N_2 mode decreases abruptly. As the plasma density increases the location of the point at which $N_{\perp r}$ changes sign, displaces towards lower Y values. For $X = 0.6$, for instance, $N_{\perp r}$ changes sign near the second EC harmonic. On the contrary, in the low density regime (see Fig. 11), one recovers another physical picture: two distinct modes (an electromagnetic and the other electrostatic) propagate separately in the EC frequency range. The electromagnetic mode (solution labelled N_1)

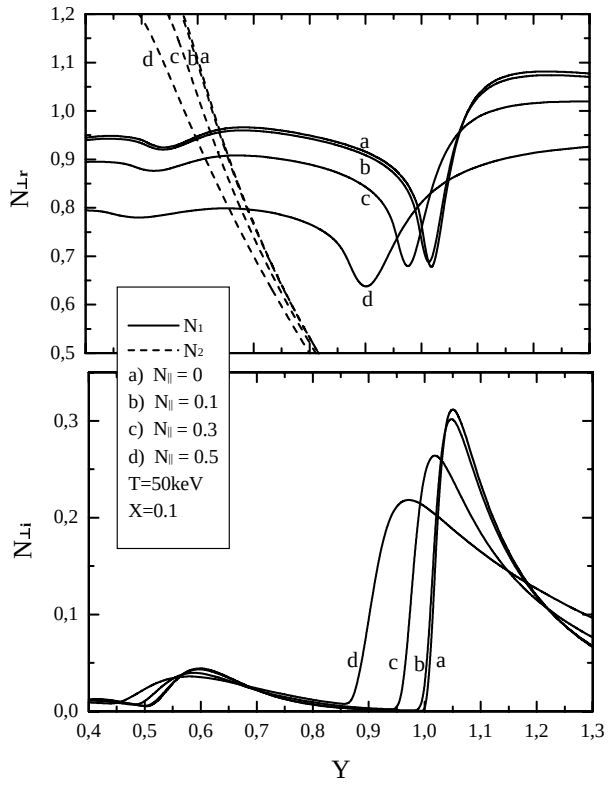

FIG. 11. As in Fig. 10 for $X = 0.1$.

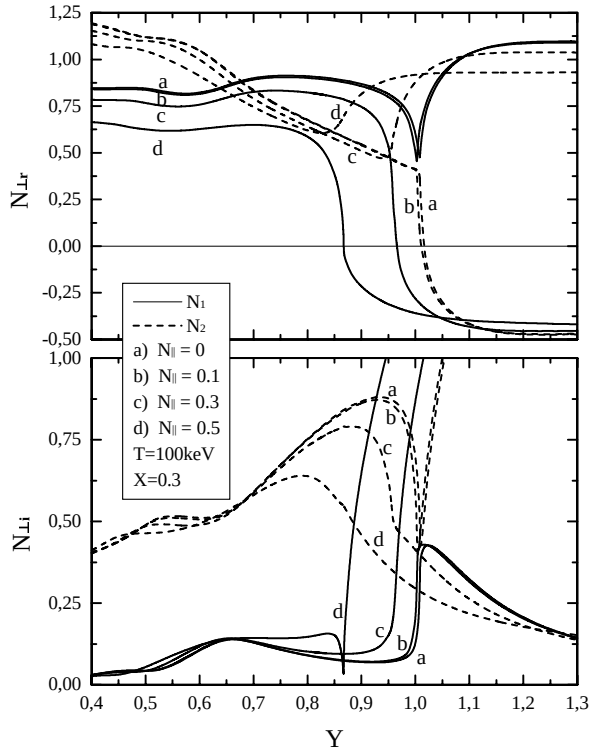

FIG. 12. As in Fig. 8 for $T = 100$ keV.

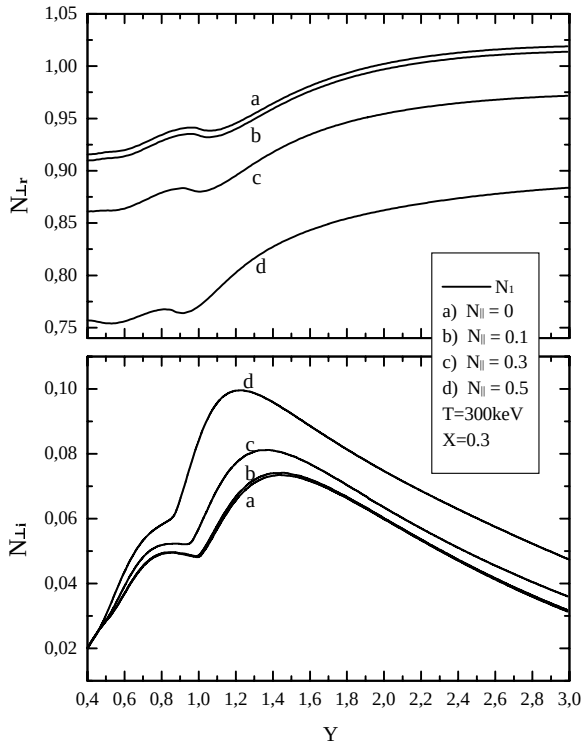

FIG. 13. As in Fig. 8 for $T = 300$ keV.

is damped near the second EC harmonic and especially, near the fundamental EC frequency. The electrostatic mode starts (at $Y = 0.4$) as an efficiently damped mode whose imaginary part of the perpendicular component of the wave refractive index increases with Y.

Further increase of the electron temperature leads to mode coupling at the fundamental EC frequency. Namely, near the ECR the high-frequency branch of the solution labelled N_1 links to the low-frequency branch of the solution labelled N_2 and vice versa, N_2 interchanges with N_1. This phenomenon has been discussed within the weakly relativistic approximation for perpendicular wave propagation [6]. In Fig. 12 we show the variation of $N_{\perp r}$ and $N_{\perp i}$ with Y for $X = 0.3$ $T = 100$ keV, and several values of $N_{||}$. As one can see, for $N_{||} = 0$ and $N_{||} = 0.1$ instead of changing its sign, the real part of the perpendicular wave refractive index of the solution labelled N_1 has a deep minimum after which it grows, following the former solution trajectory of the other mode. Simultaneously, the solution labelled N_2 starts to decrease following the former solution trajectory of N_1. Further increase of the electron temperature enlarges the $N_{||}$ - range in which the interchange of the solution trajectories occurs. We note in passing that the expression for the location of this branch point given in [7] is not correct.

In the fully relativistic range of temperatures the mode coupling and all harmonic structure is washed out. This can be verified in Fig. 13 on which we have represented the variation of $N_{\perp r}$ and $N_{\perp i}$ with Y for $X = 0.3, T = 300$ keV, and several values of $N_{||}$. We see that only solutions describing the electromagnetic mode persist. The variation of $N_{\perp r}$ with Y is smooth. The wave damping is significant. The imaginary part of the wave refractive index increases with increasing $N_{||}$ and near the ECR it attains $N_{\perp i} \simeq N_{\perp r}/10$.

V Conclusions

We have investigated waves propagating at an arbitrary angle with respect to the steady magnetic field, in relativistic thermal plasma. The present paper completes our previous work [3] in which

waves propagating perpendicularly to the magnetic field in relativistic plasma, have been studied. The dispersion relation governing waves propagating in homogeneous relativistic plasma confined by steady magnetic field has been solved numerically in a wide range of plasma parameters and wave propagation conditions. Firstly, we have examined the temperature and $N_{||}$ -dependence of the location of the plasma cutoff of the O mode. It is concluded that in a wide $N_{||}$-range ($0 \leq N_{||} < 1$) the temperature increase leads to an important increase of the plasma cutoff density. The obtained numerical results reveal that the so-called relativistic and Doppler regimes of EC wave propagation can not be separated clearly by some distinguishing features. A clear difference between these regimes can be observed only in the wave absorption properties or more precisely, in the wave absorption profiles. The obtained results show an anomalous wave dispersion near the fundamental and second harmonics of the EC frequency. This effect is very pronounced at low electron temperatures. In the high-temperature ($T \geq 300$ keV), fully relativistic domain, it disappears gradually. The damping of O modes propagating in thermal relativistic plasma is efficient. The maximum value of the imaginary part of the wave refractive index attains relatively high values, $N_{\perp i} \leq N_{\perp r}/10$. As expected, at low electron temperatures the absorption profiles show a harmonic structure which as the electron temperature increases, gradually transforms into quasi-continuous spectrum. Note that when the electron density is increased, the imaginary part of the wave refractive index starts to increase up to a broad maximum occurring at high densities.

The results of the X mode propagation and absorption recover another physical picture. This mode is more strongly coupled to the plasma than the O mode and new phenomena induced by relativistic effects are found. It is shown that the interaction of X and QL modes which as discussed in previous theoretical studies, can take place near the second EC harmonic, in fact is limited to a relatively low temperature range. In the intermediate temperature range mode interaction may occur near the EC frequency. Here it is found that this phenomenon occurs also for oblique wave propagation. In the fully relativistic temperature range there is no mode coupling phenomena. The X mode is efficiently damped near the second and especially, near the first EC harmonic. High damping rates characterize the quasi-longitudinal mode propagation and absorption. Finally, we note that some of the observed propagation and absorption properties may be attractive for future applications in devices with energetic electrons.

References

[1] Batchelor D.B., Goldfinger R.C. and Weitzner H., Phys. Fluids **27** (1984) 2835.

[2] Bornatici M. and Ruffina U., Plasma Phys. Contr. Fusion **30** (1988) 113.

[3] Pešić S. and Nikolić Lj., Engineering Physics Series, Publications of the Faculty of Electrical Engineering (1997) p.26, Belgrade.

[4] Nikolić Lj. and Pešić S., Plasma Phys. Contr. Fusion **40** (1998).

[5] Gradshteyn I.S. and Ryzhik I.A., Table of Integrals, Series and Products, Academic Press (1980), New York.

[6] Bindslev H., Plasma Phys. Control. Fusion **35** (1993) 1093.

[7] Lazzaro E. and Ramponi G., Plasma Phys. **23** (1981) 53.

[8] Bornatici M., Engelmann F., Maroli C. and Petrillo V., Plasma Phys. **23** (1981) 89.

[9] Pešić S., Phys. Fluids **31** (1988) 115.

(Received June 1998.)